

## Micro-Transfer-Printed O-band GaAs QD III-V-on-Si DFB Laser

Jing Zhang<sup>1,2\*</sup>, Igor Krestnikov<sup>3</sup>, Ruggero Loi<sup>4</sup>, Peter Ossieur<sup>5</sup>, Guy Lepage<sup>6</sup>, Peter Verheyen<sup>6</sup>, Joris Van Campenhout<sup>6</sup>, and Gunther Roelkens<sup>1,2</sup>

<sup>1</sup>Photonics Research Group, INTEC, Ghent University - IMEC, Ghent, Belgium

<sup>2</sup>Center for Nano- and Biophotonics, Ghent University - IMEC, Ghent, Belgium

<sup>3</sup>Innolume GmbH, Konrad-Adenauer-Allee 11, 44263 Dortmund, Germany

<sup>4</sup>X-Celeprint Ltd, Lee Maltings, Dyke Parade, Cork, Ireland

<sup>5</sup>IDLab, INTEC, Ghent University - IMEC, Ghent, Belgium

<sup>6</sup>IMEC, Kapeldreef 75, 3001 Heverlee, Belgium

\* jingzhan.zhang@ugent.be

We present an array of GaAs QD III-V-on-Si DFB lasers integrated by micro-transfer printing. An alignment tolerant III-V/Si taper structure is used to evanescently couple light from the laser cavity to the underlying 400 nm thick rib waveguide. Single mode operation around 1300 nm with 48 dB side mode suppression ratio and a waveguide-coupled power of 0.5 mW is demonstrated.

**Keywords:** Silicon Photonics, Distributed Feedback Laser, Micro-Transfer Printing, Heterogeneous Integration

### INTRODUCTION

Driven by the ever-increasing data traffic, giant data centers have been built in the past few years. In order to connect the servers in these data centers, significant volumes of optical transceivers with high reliability, low-power consumption and low-cost are heavily demanded. Silicon photonics (SiPh) is the most promising contender to meet this demand due to its high-index contrast and CMOS compatibility, which allows for the realization of compact photonic integrated circuits (PICs) on 200 mm or 300 mm wafers in a high-volume and at low cost. Yet, the absence of integrated laser sources is a significant obstacle in reducing the cost. Different approaches have been explored to cope with this challenge by combining the advantages of III-V materials and SiPh. Amongst these approaches, die/wafer-to-wafer bonding has been developed as a commercial solution [1], however it requires the development of dedicated III-V processes in a CMOS fab. Hetero-epitaxial growth is acknowledged as an ultimate solution and experienced significant progress in recent years, but advances in material quality are still needed and similarly III-V processing in a CMOS fab needs to be developed[2]. An alternative is the use of micro transfer printing, which decoupled the processing of the III-V semiconductors and that of the silicon photonics and allows for the integration of device coupons released from the native substrate onto a target substrate in a massively parallel way. Quantum dot lasers (QD lasers) have attracted intense interest in recent years due to their superior characteristics, such as low linewidth enhancement factor, temperature stability, high flexibility in gain bandwidth and emission wavelength engineering etc. [3]. In this work, we developed a process flow for the integration of GaAs QD laser devices on a SiPh platform using micro-transfer printing. Following this process flow we demonstrate an array of evanescently coupled O-band GaAs QD on Si DFB lasers.

### DESIGN and FABRICATION

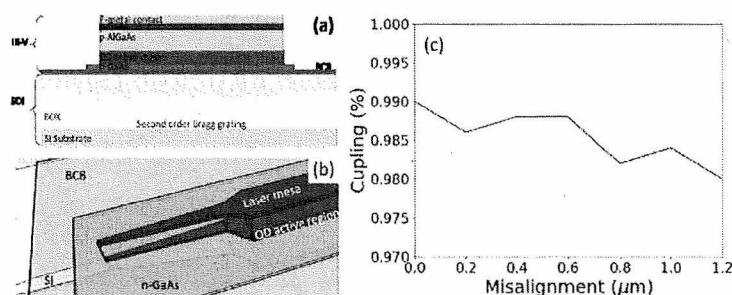


Fig. 1. (a) Schematic of the GaAs QD-on-Si DFB laser, (b) Schematic of the alignment-tolerant III-V/Si taper structure, (c) Simulated coupling efficiency as a function of lateral misalignment.

The Si waveguide circuits used in this work were fabricated at imec, by 193nm Deep-UV lithography and a 180 nm single-step etch into a 400nm thick Si device layer. Fig. 1(a) shows the schematic of the GaAs QD/Si DFB laser cavity, which has a hybrid waveguide structure where a III-V waveguide is overlaid on a uniform second-order Bragg grating

with a thin layer of DVS-BCB in between. The Bragg grating is patterned on a  $9\ \mu\text{m}$  wide rib waveguide and the length, period and duty cycle of it are  $700\ \mu\text{m}$ ,  $390\ \text{nm}$  and  $75\%$ , respectively. The overall length of the GaAs QD structure is  $1660\ \mu\text{m}$  long, which consists of a straight III-V rib waveguide with a  $2\ \mu\text{m}$  wide p-mesa and a  $6\ \mu\text{m}$  wide QD active region, and a pair of two-level III-V/Si taper structures at each side to couple the optical power to the underlying Si waveguides, as shown in Figure 1(b). This taper structure shows excellent lateral alignment tolerance as shown in Fig.1(c), for the case of a  $30\ \text{nm}$  thick DVS-BCB bonding layer, which is able to accommodate the alignment accuracy that a state-of-the-art micro-transfer printing tool can obtain ( $<1\ \mu\text{m}$  @  $3\sigma$ ). As a trade-off, its overall length is  $310\ \mu\text{m}$ .

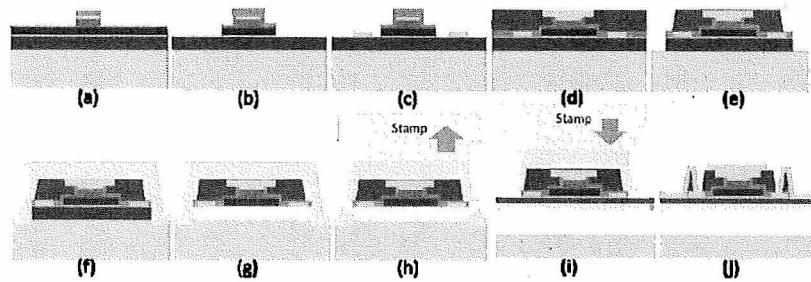


Fig. 2. Process flow for the definition of the GaAs QD SOA structures on the native GaAs substrate. (a-b) Rib waveguide definition, (c) n-contact metal deposition, (d) BCB planarization and p-contact metal deposition, (e) coupon mesa definition, (f) photoresist encapsulation and tether definition, (g) release etch, (h-i) Micro-transfer printing of GaAs QD device coupons, (j) final metallization.

The GaAs QD epitaxial structure used in this work was grown by Innolume. It consists of 11 QD layers interleaved with GaAs spacer layers, a  $200\ \text{nm}$  thick p-GaAs contact layer, a  $670\ \text{nm}$  thick p- $\text{Al}_{0.8}\text{Ga}_{0.2}\text{As}$  cladding and, a  $250\ \text{nm}$  thick n-GaAs contact layer and a  $1\ \mu\text{m}$  thick  $\text{Al}_{0.95}\text{Ga}_{0.05}\text{As}$  release layer. The dimensions of the GaAs device coupons are  $40\ \mu\text{m}$  by  $1700\ \mu\text{m}$ . The process flow of the fabrication and release of the GaAs QD device coupons and their micro-transfer printing on the target SiPh substrate is described in Fig. 2. The p-cladding mesa is defined by electron beam lithography with a hydrogen silsesquioxane (HSQ) resist and ICP dry etching (Fig.2(a)), followed by the other ICP dry etching with a SiN hard mask to pattern the QD active layers (Fig.2(b)). Then the n-contact metal stack layer is deposited (Fig.2(c)). After planarising the III-V waveguide structures using a thick BCB layer and p-contact metal deposition (Fig.2(d)), the coupon is defined by a combination of RIE etch and ICP etch into the GaAs substrate (Fig.2(e)). The coupon is then encapsulated with a thick photoresist layer (Fig.2(f)) and ready for release etching. A room temperature  $1:1\ 37\%$  HCl:DI solution is used to selectively etch the release layer (Fig.2(g)). On the SiPh substrate a thin BCB layer is spin-coated and is then baked at  $150\ ^\circ\text{C}$  for 15 minutes. Next, a PDMS stamp with a post size similar to that of the device is used in the micro-transfer printing process to pick-up the device up from the donor III-V substrate and to transfer print it onto the SiPh substrate (Fig.2(h,i)). Finally, a few simple steps of photoresist encapsulation layer removal, BCB curing and metal deposition are performed to allow electrical contact of the device (Fig.2(j)).

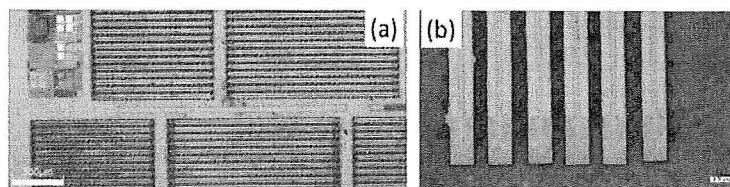


Fig. 3. (a) Microscope image of the released GaAs device coupons, (b) Bottom surface of the released coupons.

Fig. 3(a) shows a microscope image of the GaAs device coupon arrays after release etching, where a dummy coupon without tether structures was detached from the substrate, indicating the completion of the undercut of the coupons. Before the micro-transfer printing process, an array of coupons was picked up manually using a piece of scotch tape. It reveals a flat and smooth bottom surface as shown in Fig.3(b), which ensures a high yield micro-transfer printing. An X-Celeprint  $\mu\text{TP-100}$  lab-scale tool was used for the transfer printing process. 5 out of 6 coupons were successfully printed on a SiPh substrate and the only failure was caused by a local particle contamination. Fig. 4(a) shows the transfer-printed GaAs QD devices after removing the photoresist encapsulation using an RIE oxygen plasma. Fig.4(b) shows the fabricated DFB lasers with metal contact pads and Fig. 4(c) shows the cross-section of the III-V/Si hybrid waveguide structure with a  $2\ \mu\text{m}$  wide p-AlGaAs mesa, a  $6\ \mu\text{m}$  wide QDs waveguide and a  $9\ \mu\text{m}$  wide underlying Si rib waveguide. The thickness of the resulting BCB bonding layer is less than  $20\ \text{nm}$  and the

alignment accuracy for each coupon is  $<1 \mu\text{m}$ . Unfortunately, the p-AlGaAs was attacked in the taper section during a wet etching step (Fig.4(d)), which introduces optical loss in the structure.

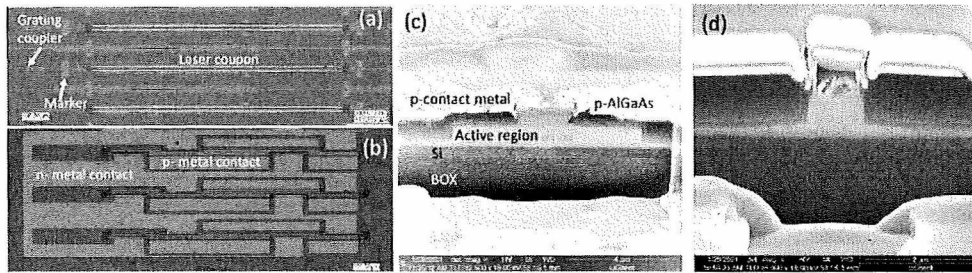


Fig. 4. Microscope image of (a) a Si PIC with micro-transfer-printed GaAs device coupons and (b) the resulting DFB lasers; (c) Focused Ion Beam cross section of the hybrid waveguide, (d) Focused Ion Beam cross section at the taper section, showing a perfect alignment but a damage in the p-AlGaAs cladding layer.

## CHARACTERIZATION

The characterization of the fabricated devices was carried out on a temperature-controlled stage at  $20^\circ\text{C}$ . A Keithley current source with a pair of DC probes was used to apply the bias current onto the devices. A standard single mode fiber was used to collect the output power from a grating coupler. It is then connected to a fiber splitter with one channel feeding into a power meter and the other connected to an optical spectral analyzer. Fig. 5(a) shows the measured I-V response and the calculated differential resistance, which reduces with the increase of bias current and reaches  $5 \Omega$  at  $140 \text{ mA}$ . As shown in Fig.5(b), the maximum single-side waveguide-coupled output power is above  $0.5 \text{ mW}$ , which is obtained by calibrating out the loss of the fiber grating coupler and fiber links. The threshold current is below  $40 \text{ mA}$ . The relatively low power is caused by the imperfect III-V taper structure, where the p-AlGaAs was attacked in the fabrication, as shown in Fig.4(d). Single mode operation at  $1300 \text{ nm}$  with a maximum side mode suppression ratio (SMSR) of  $48 \text{ dB}$  was demonstrated, as the superposed spectra show in Fig.5(c).

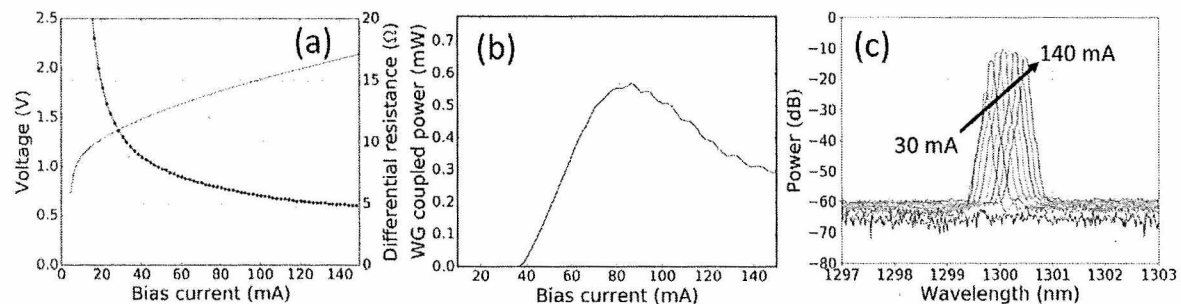


Fig. 5. Performance of a representative GaAs QD on Si DFB laser at  $20^\circ\text{C}$ . (a) V-I curve and differential resistance, (b) P-I curve (c) Superposition of the output spectra with the increase of the applied bias current.

## CONCLUSION

We developed the process flow for the fabrication and release of GaAs QD device coupons on a GaAs source wafer. These device coupons were successfully transfer-printed on a SiPh substrate. The demonstrated DFB lasers show single mode operation at  $1300 \text{ nm}$  with  $48 \text{ dB}$  side mode suppression ratio. Although the output power of the fabricated device is not ideal, this demonstration verified the feasibility of the integration of GaAs QD lasers on a SiPh platform using micro-transfer printing.

Acknowledgements: This work was supported by the European Union's Horizon 2020 research and innovation programs under agreement 825453 (CALADAN).

## References

- [1] R. Jones et al., "Heterogeneously Integrated InP-Silicon Photonics: Fabricating Fully Functional Transceivers," IEEE Nanotechnology Magazine, vol. 13, no. 2, pp. 17-26, April 2019.
- [2] Y. Shi et al., "GaAs Nano-Ridge Lasers Epitaxially Grown on Silicon," Ph.D thesis, Ghent University, 2020.
- [3] G. Frédéric et al., "Physics and applications of quantum dot lasers for silicon photonics," Nanophotonics, vol. 9, no. 6, pp. 1271-1286, 2020.
- [4] B. Corbett et al., "Transfer Printing for Silicon Photonics", Semiconductors and Semimetals, vol. 99, pp.43-70, 2018